Chinese Chemical Letters 34 (2023) 107725

Contents lists available at ScienceDirect

Chinese Chemical Letters

journal homepage: www.elsevier.com/locate/cclet

A simple fluorescent sensor for highly sensitive detection of UO_2^{2+}

Huanhuan Ding[a], Chenguang Li[a], Hailing Zhang[a], Na Lin[a], Wen-Sheng Ren[a], Shicheng Li[a], Weidong Liu[a], Zhonghua Xiong[a], Binyuan Xia[a,*], Chong-Chen Wang[b,*]

[a] Institute of Materials, China Academy of Engineering Physics, Mianyang 621907, China
[b] Beijing Key laboratory of Functional Materials for Building Structure and Environment Remediation/Beijing Energy Conservation & Sustainable Urban and Rural Development Provincial and Ministry Co-construction Collaboration Innovation Center, Beijing University of Civil Engineering and Architecture, Beijing 100044, China

ARTICLE INFO

Article history:
Received 5 April 2022
Revised 16 July 2022
Accepted 3 August 2022
Available online 5 August 2022

Keywords:
Uranyl ion
Trace analysis
Aggregation-induced emission
Fluorescent sensor
Intramolecular charge transfer

ABSTRACT

Extensive application of nuclear energy has caused widespread environmental uranium contamination. New detection approaches without complicated sample pretreatment and precision instruments are in demand for on-site and in-time determination of uranyl ions in environmental monitoring, especially in an emergency situation. In this work, a simple and effective fluorescent sensor (*Z*)-*N*'-hydroxy-4-(1,2,2-triphenylvinyl)benzimidamide (TPE-A) with aggregation-induced emission (AIE) character was established and studied. It could realize to detect UO_2^{2+} *via* quenching the fluorescence of its aggregation-induced emission, with good selectivity and sensitivity. Such strategy shows a wide linear range from 5.0×10^{-8} mol/L to 4.5×10^{-7} mol/L ($R^2 = 0.9988$) with exceptional sensitivity reaching 4.7×10^{-9} mol/L, which is far below the limit for uranium in drinking water (30 μg/L, *ca.* 1.1×10^{-7} mol/L) stipulated by the WHO. A response time less than four minutes make it rapid for uranyl ion measurement. It was applied for detection of uranyl ion in spiked river water samples with recoveries in the range of 98.7%-104.0%, comparable to those obtained by ICP-MS. With the advantages of portable apparatus, rapid detection process and high sensitivity, TPE-A can serve as a promising fluorescent sensor for the detection of UO_2^{2+} in environmental water samples.

Uranium is a toxic and radioactive nuclide, which is widely applied in civil and military nuclear fields [1,2]. Human exposure to uranium has reported to result in a series of health problems, such as cancer, renal system ailments and genetic diseases [3,4]. As the growing utilization of nuclear energy, especially the occurrence of undesirable nuclear accidents, uranium contamination is widely found in natural waters, such as river [5], groundwater [6] and ocean [7]. The pollution of uranium in environment water has become a social concern. Thus, it is of great significance to detect the concentration of uranium in aqueous environment.

Uranium is usually associated with oxygen, forming various oxidation states (*i.e.* +2, +3, +4, +5, +6), and uranyl ion (UO_2^{2+}) is the most stable chemical form in aqueous environment. Until now, routine methods for the trace level uranyl detection mainly include inductively coupled plasma mass spectrometry (ICP-MS) [8], inductively coupled plasma optical emission spectrometry (ICP-OES) [9], atomic emission spectroscopy (AES) [10] and surface-enhanced Raman scattering (SERS) [11]. Although these techniques are sensitive and reliable, they often require large and expensive equipments, complicated processing procedures, strict operations and relatively long analysis time, which restrict the on-site rapid detection of UO_2^{2+}. Fluorescence analysis, with the advantages of easy operation, simple apparatus, excellent sensitivity and real-time monitoring, has been received increasing attention [12]. In recent years, some organic fluorescence sensors for detecting UO_2^{2+} have been reported [13,14]. However, most of these sensors show low solubility in water and would suffer from suppressed emission or even complete fluorescence quenching in high water fractions, which limited their practical applications.

Among the fluorescence analysis techniques, fluorescence organic molecules with aggregation-induced emission (AIE) property have been shown to be particularly valuable, as first reported by Zhang *et al.* [15]. Tetraphenylenthene (TPE) moiety has been reported as an excellent fluorophore for designing of AIE sensors. To date, a variety of TPE-based fluorescent sensors have been developed and utilized, such as for Th^{4+} [16], Cu^{2+} [15] and Hg^{2+} [17]. Wen *et al.* [18] and Lin *et al.* [19] developed two TPE-based fluorescent sensors, TPE-T and TPE-BSA, respectively. The two sensors

* Corresponding authors.
E-mail addresses: ybinxia@caep.cn (B. Xia), chongchenwang@126.com (C.-C. Wang).

https://doi.org/10.1016/j.cclet.2022.08.005
1001-8417/

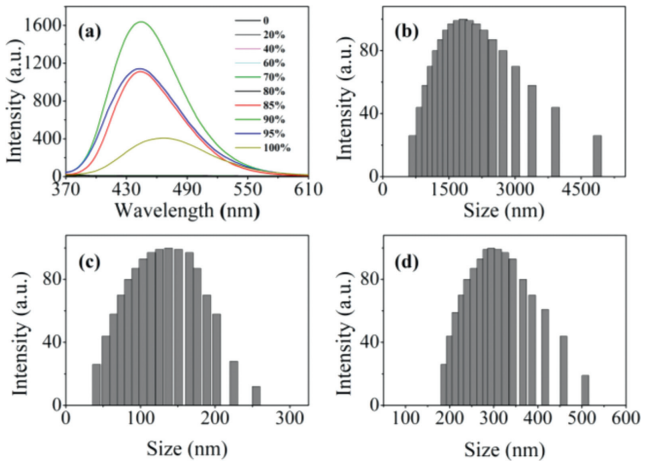

Fig. 1. (a) Fluorescence spectra of TPE-A (10 μmol/L) in H_2O/THF mixtures with f_w ranging from 0% to 100%. Dynamic light scattering results of (b) TPE-A (10 μmol/L) in H_2O/THF (90/10, v/v) mixture, (c) TPE-A (10 μmol/L) in H_2O/THF (85/15, v/v) mixture, and (d) TPE-A (10 μmol/L) with UO_2^{2+} (0.5 μmol/L) in the H_2O/THF (85/15, v/v) mixture.

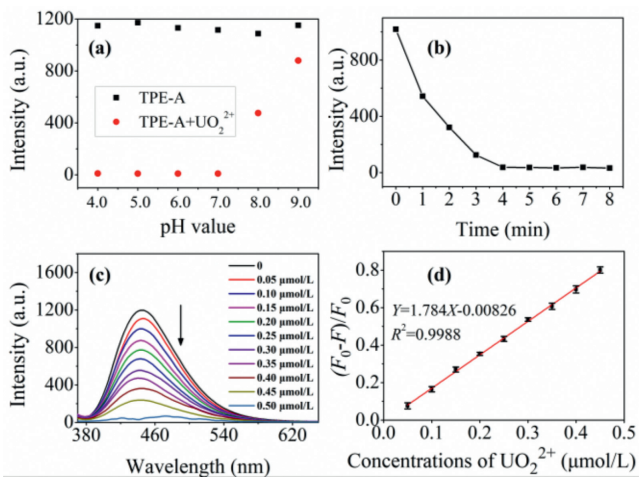

Fig. 2. (a) Fluorescence intensity of TPE-A (10 μmol/L) and TPE-A (10 μmol/L) + UO_2^{2+} (0.5 μmol/L) at 444 nm in H_2O/THF (85/15, v/v) solution at different pH. (b) The response time curve of TPE-A (10 μmol/L) to uranyl ions (0.5 μmol/L) at 444 nm in H_2O/THF (85/15, v/v) mixture at pH 7.0. (c) Fluorescence spectra of TPE-A (10 μmol/L) in the presence of different concentrations (0-0.5 μmol/L) in the H_2O/THF (85/15, v/v) solution at pH 7.0. (d) The linear plot and relationship of $(F_0\text{-}F)/F_0$ *versus* the concentrations of UO_2^{2+} (0.05-0.45 μmol/L).

monitored UO_2^{2+} with high water fractions, whereas the detection limit could not reach the levels of UO_2^{2+} in natural waters (0.31 μg/L for global rivers [20], and 3.3 μg/L for ocean [7]), approximatively nanomolar level. Therefore, to further improve the sensitivity is the key to achieve the determination of trace uranium in the environment.

Amidoxime group (–C(NH_2)=N-OH), which has been reported to be used for uranium extraction from seawater, is one of the best groups to adsorb UO_2^{2+} from aqueous solution and reveals strong affinity for UO_2^{2+} [13,21,22]. Herein, a novel and sensitive fluorescence sensor (TPE-A) is developed through a synthesis of tetraphenylenthene fluorophore with amidoxime group. It is demonstrated that this sensor system could greatly improve the fluorescence detection sensitivity reaching 4.7×10^{-9} mol/L, attributed to the promoted adsorption ability of amidoxime groups to UO_2^{2+}. In addition, analytical application of the method for determination of UO_2^{2+} in FuJiang River samples was successfully conducted, which showed that TPE-A could be a sensitive and convenient fluorescent sensor for trace UO_2^{2+} detection.

Details of TPE-A synthesis, characterization methods, spectroscopic and adsorption measurements are described in Supporting information.

The AIE fluorescence characteristic of TPE-A was studied in H_2O/THF (from 0 to 1, v/v) with various water volume fractions (f_w). Fig. 1a shows the emission of TPE-A in various H_2O/THF mixtures. When the water fraction increases from 0% to 80% (Fig. S5 in Supporting information), the fluorescence intensity at 444 nm remains almost unchanged. While the water content reaches 85%, the fluorescence intensity of TPE-A increases significantly, and gets to its climax when the water content reaches 90%. The fluorescence intensity of the mixture ($f_w = 90\%$) increases by 147-fold compared to the TPE-A in mixture ($f_w = 0\%$). TPE-A aggregates in aqueous solutions with high water fractions since it is soluble in THF and poorly soluble in water. In dispersed solution, the fluorophores emit almost no light caused by their rotation or twisting motions against each other with the solvent media transforms the photonic energy to thermal energy. Upon aggregate formation, the emission of TPE-A is induced or rejuvenated by the restriction of intramolecular motions (RIM) [23,24]. When f_w increases from 90% to 100%, the fluorescence intensity decreases, because TPE-A may agglomerate rapidly to form amorphous materials with decreased emission [25].

To confirm the presence of aggregates, particle size distribution analyses (Figs. 1b–d) were performed on dynamic light scattering (DLS) experiments. As shown in Figs. 1b and c, nanoparticles with an average size of *ca.* 1822.1 nm ($f_w = 90\%$) and 137.6 nm ($f_w = 85\%$) are observed, respectively, which suggests the formation of fluorescent aggregates of TPE-A. Moreover, the stability test of the fluorescent sensor was conducted to evaluate the performance. It is observed that the fluorescence intensity of the mixture ($f_w = 85\%$) at 444 nm stays almost constant in 600 s, while the fluorescence intensity of the mixture ($f_w = 90\%$) fluctuates continually and enhances dramatically at 323 s (Fig. S6 in Supporting information), indicating the mixture ($f_w = 90\%$) is unstable. Then, flocculent precipitation is observed after 10 min (Fig. S7 in Supporting information). Considering the stability, the water fraction ($f_w = 85\%$) would be chosen as the optimum condition for detecting experiments of UO_2^{2+}.

The fluorescence properties of the sensor are affected by the pH. As shown in Fig. 2a, the effect of pH value was studied in the range of 4.0 to 9.0. TPE-A exhibits strong fluorescence intensity in the absence of UO_2^{2+} at different pH values (from 4.0 to 9.0). After addition of 0.5 μmol/L UO_2^{2+}, the emission of TPE-A (10 μmol/L) could be quenched remarkably under acidic and neutral conditions, while quenched only 56.3% at pH 8.0 and 23.6% at pH 9.0 (Table S1 in Supporting information), which may be due to some uranyl exists in the form of anions in alkaline conditions (Fig. S8a in Supporting information). Considering the rigorous operation under acidic condition, neutral condition (pH 7.0) is chosen as the optimal experimental condition.

In order to study the response time of TPE-A to UO_2^{2+}, the fluorescence intensity within 8 min was recorded (Fig. 2b). It can be seen that the fluorescence intensity at 444 nm stays almost constant after 4 min. The short reaction time of the TPE-A toward UO_2^{2+} might be related to the strong coordination of amidoxime group.

In order to estimate the potential of TPE-A as a sensor for the UO_2^{2+} detection, UO_2^{2+} was gradually added to H_2O/THF ($f_w = 85\%$) mixture in titration experiment. Fluorescence responses of TPE-A to UO_2^{2+} were then recorded. Fig. 2c shows the emission intensity of TPE-A in the presence of UO_2^{2+}. Notably, fluorescence intensity of the mixture decreases gradually with the concentra-

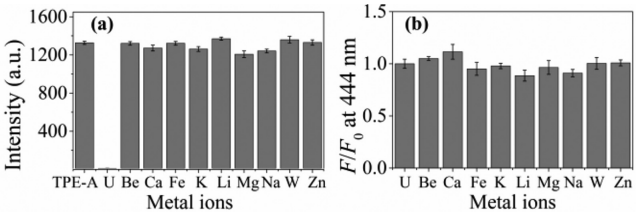

Fig. 3. (a) Fluorescence intensity of TPE-A (10 μmol/L) in H_2O/THF (85/15, v/v) solution in the presence of different metal ions (10 μmol/L). (b) A competitive binding assay with TPE-A (10 μmol/L) for UO_2^{2+} (10 μmol/L) over another metal ion (10 μmol/L). F_0: fluorescence intensity of [TPE-A+U]; F: fluorescence intensity of [TPE-A+U+another metal ion].

tion of UO_2^{2+} increases. Fig. S9 (Supporting information) shows the relationship between fluorescence intensity at 444 nm and the concentration of UO_2^{2+}. Moreover, the fluorescence quenching efficiency ($(F_0\text{-}F)/F_0$, F and F_0 are the emission intensities at 444 nm in the presence and absence of the UO_2^{2+}, respectively) exhibits a good linear relationship with the concentration of UO_2^{2+} in the range of 0.05 μmol/L to 0.45 μmol/L (Fig. 2d). The linear equation is $Y = 1.784X\text{-}0.00826$ ($R^2 = 0.9988$) with Y as the fluorescence quenching efficiency, X as the UO_2^{2+} concentration. The minimum detection limit is 4.7×10^{-9} mol/L calculated according to $LOD = 3\sigma/k$, where σ is the standard deviation of the blank measurement, and k is the slope of linear equation. The results show that the LOD is below the limit for uranium in drinking water (30 μg/L, *ca.* 1.1×10^{-7} mol/L) defined by the WHO, suggesting that TPE-A could be used as a novel fluorescence sensor for the determination of trace UO_2^{2+} in environmental samples.

The existence of UO_2^{2+} results in a gradual quenching of TPE-A emission. The Stern-Volmer plot ($F_0/F = 1 + K_{sv}Q$) was determined to evaluate the fluorescence quenching efficiency of TPE-A upon UO_2^{2+}, where F_0 and F are the fluorescence intensities in the absence and presence of UO_2^{2+}, Q is the concentration of UO_2^{2+}, and K_{sv} is the Stern-Volmer quenching constant, and the bigger K_{sv}, the better quenching efficiency. As shown in Fig. S10 (Supporting information), the plot curves upward with the increase of UO_2^{2+} concentration, indicating that TPE-A has a high quenching efficiency. The inset in Fig. S10 shows that a linear Stern-Volmer plot is obtained with a large K_{sv} of 2.76×10^6 L/mol at low concentration of UO_2^{2+}, indicating that the TPE-A has high sensitivity for uranyl ion.

Metal ions in environmental waters could interfere with the detection of UO_2^{2+}. Various common metal ions (Be^{2+}, Ca^{2+}, Fe^{3+}, K^+, Li^+, Mg^{2+}, Na^+, W^{6+}, Zn^{2+}) were selected as potential interference substances. Fluorescence quenching degrees ($1\text{-}F/F_0$) were performed in this study. As illustrated in Fig. 3a, most metal ions only cause ignorable fluorescence changes of TPE-A (by about 5%). It is noticed that Mg^{2+} quenches the fluorescence by about 9%. On the contrast, the addition of UO_2^{2+} results in almost complete fluorescence quenching of TPE-A (>99%), much higher than those of common metal ions (Table S2 in Supporting information). To further evaluate the influence of metal ions to the detection of UO_2^{2+}, competition experiments were also performed. As showed in Fig. 3b and Table S2 (Supporting information), the fluorescence intensity in the presence of UO_2^{2+} mixed with common ions is almost same with that of UO_2^{2+} alone, suggesting that the sensor has strong binding capacity among the tested metal ions. The interference and competition experiments of anions and humic acid (HA) as natural organic matter were also conducted, respectively. Fig. S11 and Table S2 (Supporting information) show the fluorescence intensity in the presence of UO_2^{2+} and HCO_3^- is higher than that of UO_2^{2+} alone, indicating that HCO_3^- may complex with uranium [26,27]. Fig. S8b (Supporting information) shows the speciation of U(VI) in the presence of bicarbonate. In alkaline conditions, HCO_3^- could easily bind with U(VI) to form $UO_2(CO_3)_2^{2-}$ and $UO_2(CO_3)_3^{4-}$, which may impede the reaction between TPE-A and UO_2^{2+} by competing for the reactive sites.

To verify the practical application of the sensor, a standard addition method was used to analyze the detection of UO_2^{2+} in Fu-Jiang River water samples. The concentration of UO_2^{2+} was determined by fluorescence spectrophotometry and ICP-MS. Table S3 (Supporting information) shows that the TPE-A sensor could be used to reliably determine the concentration of UO_2^{2+} with satisfactory recoveries (98.7%-104.0%) and relative standard deviation (RSD) values (<5%). There is good agreement between the TPE-A sensor and ICP-MS measurements. The performance of the proposed sensor was compared with some reported sensors (Table S4 in Supporting information). It was found that TPE-A could detect UO_2^{2+} in a relatively wider pH range and established a bigger quenching constant K_{sv}. More importantly, the detection limit of TPE-A could reach nanomolar level, which could be applied in practical samples in the environment.

In view of the fluorescence quenching, FTIR analyses were carried out to confirm whether the coordination between TPE-A and UO_2^{2+} occurred. Fig. S12 shows the FTIR spectra of TPE-A and U-laden TPE-A, the bands at 1641 and 906 cm^{-1} in TPE-A are indicative of the –C=N– and =N–O– of amidoxime group, respectively. The adsorption bands at 1641 and 906 cm^{-1} shift to 1646 and 927 cm^{-1} after adsorption, respectively, which indicates the coordination of TPE-A with UO_2^{2+}. The possible fluorescence quenching mechanisms are as follows: (1) after the coordination of TPE-A with UO_2^{2+}, the aggregates may dissociate, and the solubility of the complex in water may be better, leading to the decrease of fluorescence; (2) the heavy atom effect of UO_2^{2+}. To determine whether the aggregates dissociated or not after coordination with uranyl ion, particle size analysis using DLS was performed (Fig. 1d). Particles are still observed in the presence of 0.05 equiv. of UO_2^{2+} and the particles increase from *ca.* 137.6 nm to 294.2 nm. The size increase implies that the aggregates of TPE-A do not dissociate after coordination with uranyl ion.

To further understand the photophysical properties of TPE-A and [TPE-A+UO_2^{2+}], density functional theory (DFT) calculations were carried out using Gaussian 16 at the level of B3LYP/6-31+G(d), SDD-MWB60. Amidoxime group can coordinate with UO_2^{2+} *via* its electrons of N or O, leading to a strong chelating reaction for uranyl ions. Researchers have proposed several binding motifs [28–30]; while DFT results exhibit that η^2 binding motif with the N-O bond is the most stable form, confirmed by single-crystal X-ray diffraction of UO_2^{2+} complexes with acetamidoxime and benzamidoxime anions [31]. The possible coordination patterns between the sensor TPE-A and UO_2^{2+} were explored, as shown in Fig. S13 (Supporting information). The binding energy of the combination [2TPE-A+UO_2^{2+}] (−135.92 kcal/mol) is much lower than that of [TPE-A+UO_2^{2+}] (−109.27 kcal/mol), indicating that two amidoxime groups lean to bind one UO_2^{2+}. Previous studies have proved that HOMO and LUMO orbitals can describe the sites where molecules tend to lose or gain electrons in the reaction process [32,33]. The calculated energy levels and HOMO-LUMO energy gaps for the TPE-A and [2TPE-A+UO_2^{2+}] are illustrated in Fig. 4. The LUMO energy level (−2.0249 eV) in the [2TPE-A+UO_2^{2+}] is much lower than that of the TPE-A (−1.4582 eV). Before and after TPE-A combines with UO_2^{2+}, the HOMO-LUMO energy gap decreased from 3.8685 eV to 3.3383 eV. In addition, the combination of TPE-A and UO_2^{2+} seems to have strong influence on the HOMO and LUMO properties of the complexes. In the free TPE-A, the electron density of HOMO mainly locates on the TPE and amidoxime moieties and the LUMO mainly distributes on the TPE moiety. When UO_2^{2+} is coordinated to the TPE-A ligand, the electrons density on the HOMO of [2TPE-A+UO_2^{2+}] mainly locates on the TPE and amidoxime moieties, while the LUMO mainly disperses on

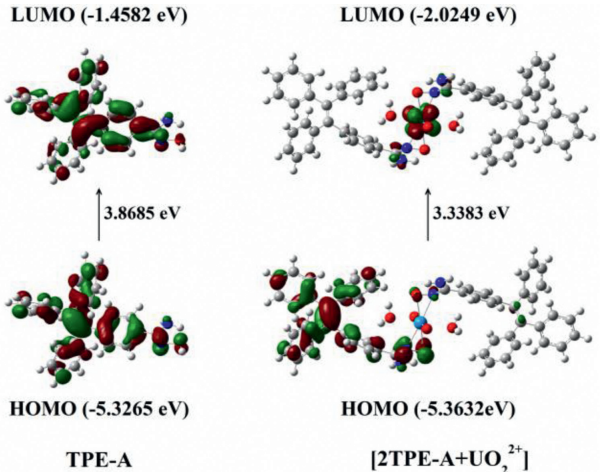

Fig. 4. Molecular orbitals of the free TPE-A ligand and [2TPE-A+ UO_2^{2+}].

the UO_2^{2+} moiety. Thus, the intramolecular charge transfer from TPE-A to UO_2^{2+} is allowed, leading to the fluorescence quenching. These results indicate that the fluorescence quenching after the addition of UO_2^{2+} is mainly due to the heavy atom effect of UO_2^{2+}.

In summary, a simple and sensitive fluorescence AIE-active sensor TPE-A has been successfully designed and synthesized for rapid uranyl ion detection in aqueous solutions. The fluorescence property of TPE-A and its application were investigated. The proposed sensor is effective with a limit of detection as low as 4.7×10^{-9} mol/L at pH 4.0-7.0. This sensor showed good accuracy in the determination of UO_2^{2+} concentrations in river water and may have potential applications for the detection of trace UO_2^{2+} in environmental systems.

Declaration of competing interest

The authors declare no financial interests/personal relationships which may be considered as potential competing interests.

Acknowledgments

We appreciate the financial support received from the National Natural Science Foundation of China (No. 21702193) and China Academy of Engineering Physics (Nos. TP03201601, TP02201711 and JMJJ20190101).

Supplementary materials

Supplementary material associated with this article can be found, in the online version, at doi:10.1016/j.cclet.2022.08.005.

References

[1] A. Bleise, P.R. Danesi, W. Burkart, J. Environ. Radioact. 64 (2003) 93–112.
[2] J. Nriagu, D.H. Nam, T.A. Ayanwola, et al., Sci. Total Environ. 414 (2012) 722–726.
[3] E.S. Craft, A.W. Abu-Qare, M.M. Flaherty, et al., J. Toxicol. Environ. Health Part B 7 (2004) 297–317.
[4] M. Yazzie, S.L. Gamble, E.R. Civitello, D.M. Stearns, Chem. Res. Toxicol. 16 (2003) 524–530.
[5] H. Windom, R. Smith, F. Niencheski, C. Alexander, Mar. Chem. 68 (2000) 307–321.
[6] O. Prat, T. Vercouter, E. Ansoborlo, et al., Environ. Sci. Technol. 43 (2009) 3941–3946.
[7] F. Endrizzi, L.F. Rao, Chem. Eur. J. 20 (2014) 14499–14506.
[8] C. Möser, R. Kautenburger, H.P. Beck, Electrophoresis 33 (2012) 1482–1487.
[9] M. Krishnakumar, G. Chakrapani, K. Satyanarayana, K. Mukkanti, J. Radioanal. Nucl. Chem. 307 (2016) 497–505.
[10] M.R. Jamali, Y. Assadi, F. Shemirani, et al., Anal. Chim. Acta 579 (2006) 68–73.
[11] S.F. Wang, S.L. Yang, H.X. Wu, et al., Sci. Bull. 64 (2019) 315–320.
[12] C.Y. Wang, C.C. Wang, X.W. Zhang, et al., Chin. Chem. Lett. 33 (2022) 1353–1357.
[13] J.Q. Ma, W.W. He, X.L. Han, D.B. Hua, Talanta 168 (2017) 10–15.
[14] A.A. Elabd, M.S. Attia, J. Lumin. 165 (2015) 179–184.
[15] S. Zhang, J.M. Yan, A.J. Qin, et al., Chin. Chem. Lett. 24 (2013) 668–672.
[16] B. Liu, Y.H. Tan, Q.H. Hu, et al., Sens. Actuators B: Chem. 296 (2019) 126675.
[17] J. Zhang, Q. Zang, F. Yang, et al., J. Am. Chem. Soc. 143 (2021) 3944–3950.
[18] J. Wen, Z. Huang, S. Hu, et al., J. Hazard. Mater. 318 (2016) 363–370.
[19] N. Lin, W.S. Ren, J.N. Hu, et al., Dyes Pigments 166 (2019) 182–188.
[20] M.R. Palmer, J.M. Edmond, Geochim. Cosmochim. Acta 57 (1993) 4947–4955.
[21] C.W. Abney, R.T. Mayes, T. Saito, et al., Chem. Rev. 117 (2017) 13935–14013.
[22] Y. Yuan, S. Zhao, J. Wen, et al., Adv. Funct. Mater. 29 (2019) 1805380.
[23] H. Zhang, J. Liu, L. Du, et al., Mater. Chem. Front. 3 (2019) 1143–1150.
[24] J. Mei, N.L.C. Leung, R.T.K. Kwok, et al., Chem. Rev. 115 (2015) 11718–11940.
[25] H. Tong, Y.Q. Dong, M. Haübler, et al., Chem. Commun. 2006 (2006) 1133–1135.
[26] J. Duan, H. Ji, X. Zhao, et al., Chem. Eng. J. 393 (2020) 124692.
[27] J. Duan, H. Ji, T. Xu, et al., Chem. Eng. J. 406 (2021) 126752.
[28] A.Y. Zhang, T. Asakura, G. Uchiyama, React. Funct. Polym. 57 (2003) 67–76.
[29] G.X. Tian, S.J. Teat, Z.Y. Zhang, L.F. Rao, Dalton Trans. 41 (2012) 11579–11586.
[30] J.L. Wang, S.T. Zhuang, Rev. Environ. Sci. Bio/Technol. 18 (2019) 437–452.
[31] S. Vukovic, L.A. Watson, S.O. Kang, et al., Inorg. Chem. 51 (2012) 3855–3859.
[32] X.H. Yi, H. Ji, C.C. Wang, et al., Appl. Catal. B: Environ. 293 (2021) 120229.
[33] C. Zhao, J. Wang, X. Chen, et al., Sci. Total Environ. 752 (2021) 141901.